

Supplementary Information

Solvent-Free Preparation of Uniform Styrene/Maleimide Copolymer Microspheres from Solid Poly(styrene-*alt*-maleic anhydride)

*Chuxuan Chen,^a Can Xu,^a Jiaxin Zhai,^a Yuhong Ma,^{a,b} Changwen Zhao,^{*a} and Wantai Yang ^{*a,b,c}*

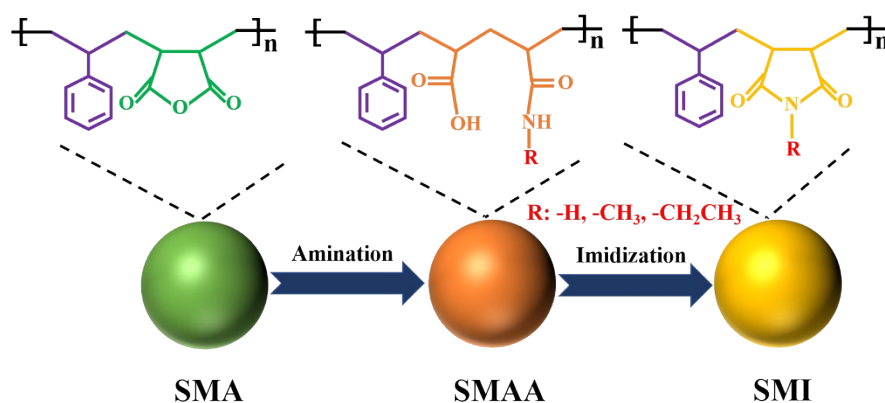
^aState Key Laboratory of Chemical Resource Engineering, Beijing University of Chemical Technology, Beijing, 100029, China

^bBeijing Engineering Research Center for the Synthesis and Applications of Waterborne Polymers, Beijing University of Chemical Technology, Beijing, 100029, China

^cKey Laboratory of Carbon Fiber and Functional Polymers Ministry of Education, Beijing University of Chemical Technology, Beijing, 100029, China

Table S1. The element content of SMA (%^a was mass percent, %^b was mole percent).

Sample	C% ^a	N% ^a	H% ^a	O% ^a	MAH% ^b
226 nm	70.39	0.03	5.47	24.11	0.50
452 nm	69.91	0.05	5.81	24.23	0.50
534 nm	70.84	0.06	5.24	23.86	0.50
728 nm	70.8	0.01	5.36	23.83	0.50



Scheme S1. Chemical route for imidization of SMA microspheres.

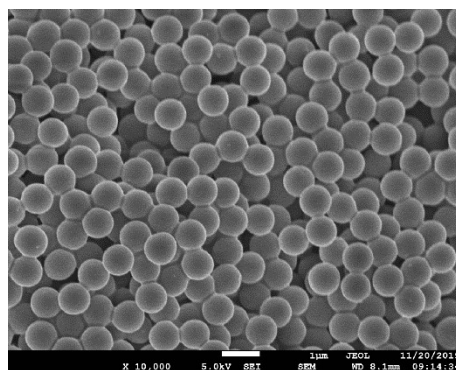


Fig. S1. SEM image of SMA microspheres. (reaction medium was the mixture of butanone and cyclohexane, butanone/cyclohexane=4/1, V/V).

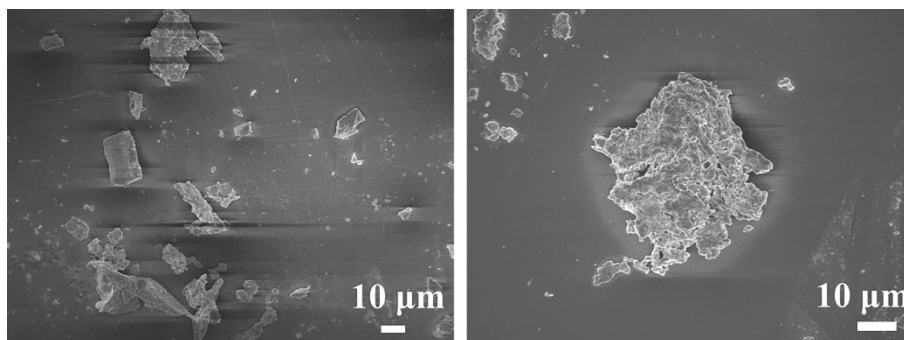


Fig. S2. SEM images of SMA prepared by solution polymerization at different magnification.

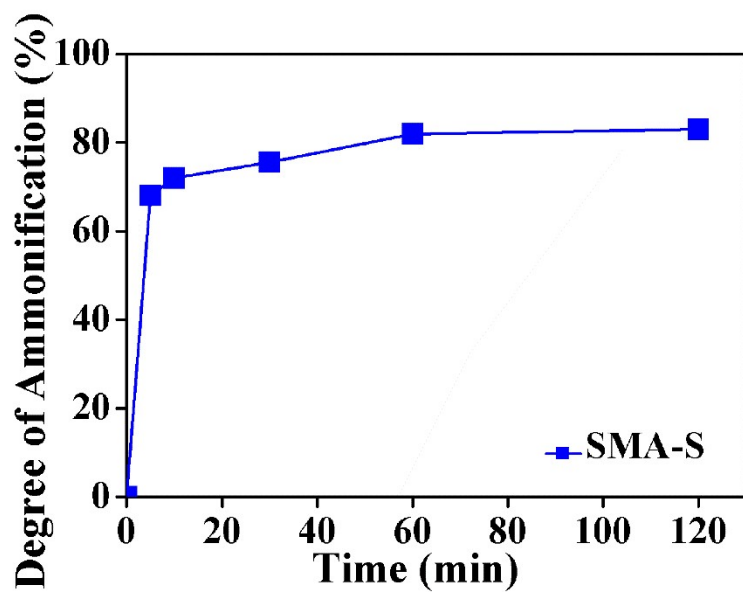


Fig. S3. The ammonification curve of SMA prepared by solution polymerization.

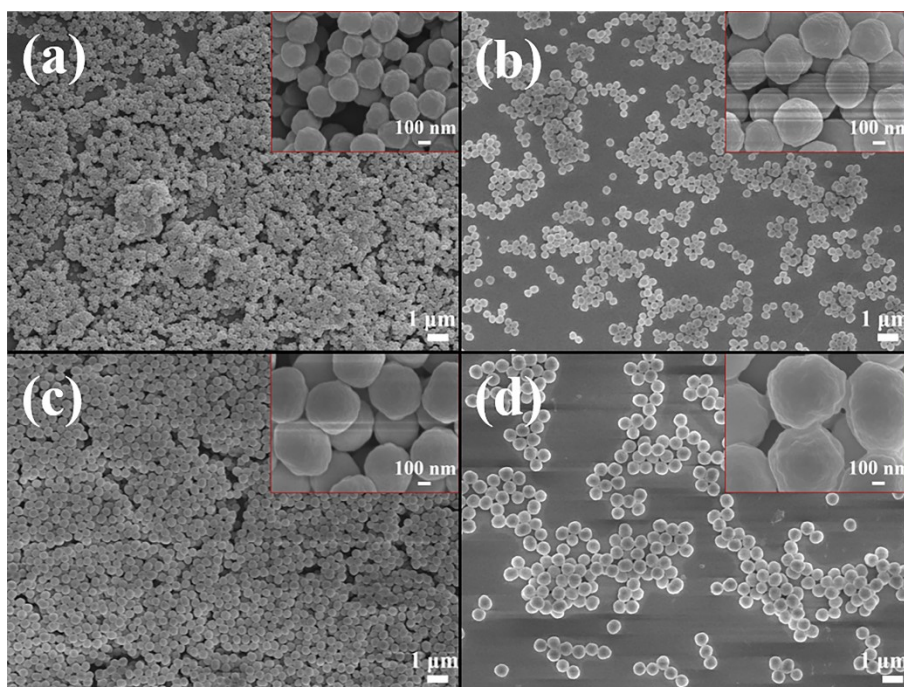


Fig. S4. SEM images of *N*-methyl SMAA. (a) 226 nm, (b) 452 nm, (c) 534 nm, and (d) 728 nm.

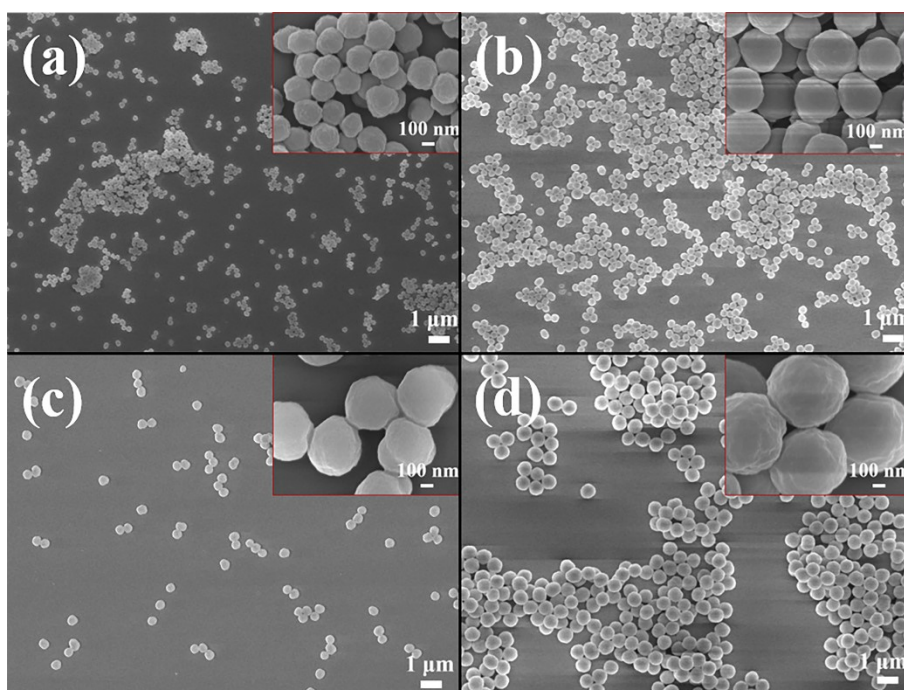


Fig. S5. SEM images of *N*-ethyl SMAA. (a) 226 nm, (b) 452 nm, (c) 534 nm, and (d) 728 nm.

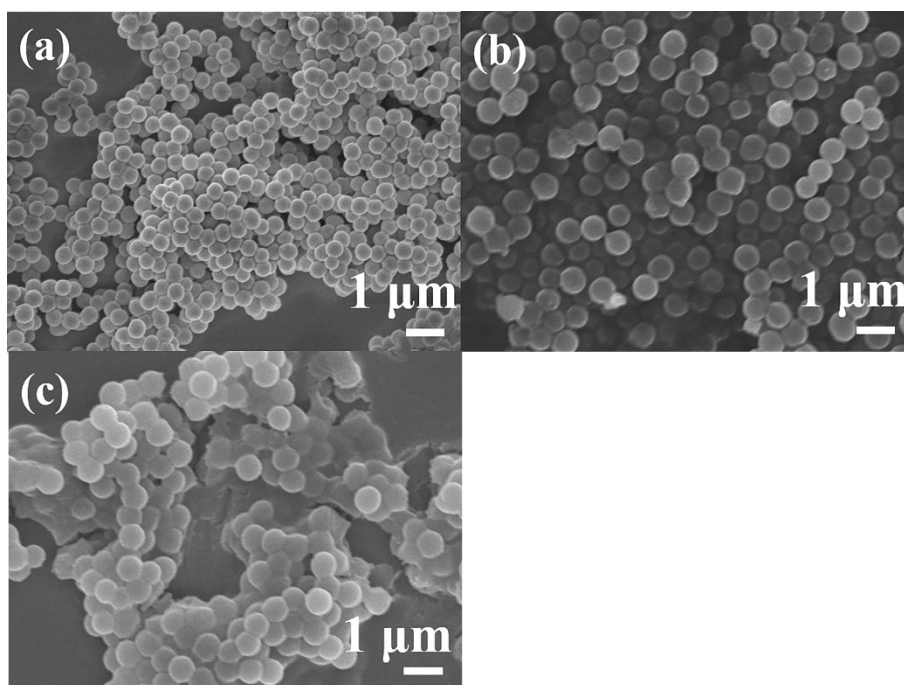


Fig. S6. SEM images of 452 nm SMA microspheres (a), 704 nm *N*-ethyl SMAA microspheres (b) and 704 nm *N*-ethyl SMI microspheres (c).

Table S2. Peak position of the groups in FTIR spectra (SMI).

SMI	C=O (imide I)	C-N-C (imide II)	Ring of imide (imide III)
NH ₃	1780;1710	1356	1180
<i>N</i> -methyl	1780;1710	1387	1130
<i>N</i> -ethyl	1780;1710	1405;1356	1130

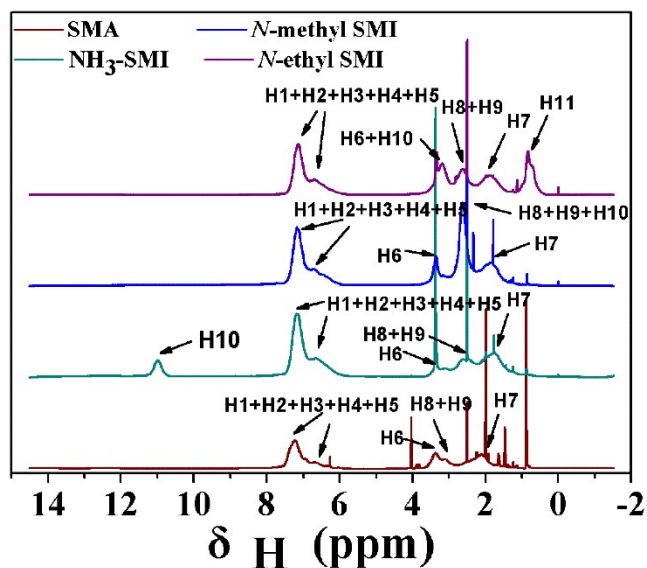


Fig. S7. ^1H NMR spectra of SMA, NH_3 -SMI, *N*-methyl SMI and *N*-ethyl SMI.

The ^1H NMR spectra of SMA and SMI are shown in Fig. S6. The signal 3.22 - 2.75 ppm of -CH- in maleic anhydride shift to 2.94 - 2.24 ppm in maleimide. From the spectra, it is obvious to find the differences between the three types of SMI. The signal 11.2 - 10.7 ppm in spectra of NH_3 -SMI was the chemical shift of N-H. The signal 1.16 - 0.27 ppm in spectra of *N*-ethyl SMI was the chemical shift of $-\text{CH}_3$ in ethyl ($-\text{N}-\text{CH}_2-\text{CH}_3$). The chemical shift (2.94 - 2.24 ppm) of *N*-methyl SMI was strongest among these SMI, which may be related to methyl group in the maleimide ring ($-\text{N}-\text{CH}_3$). The rest signals in these spectra were the chemical shift of H in benzene ring (6.10 - 7.60 ppm), -CH- (3.08 - 3.60 ppm) and $-\text{CH}_2-$ (1.21 - 2.18 ppm) in styrene, these signals were almost same.

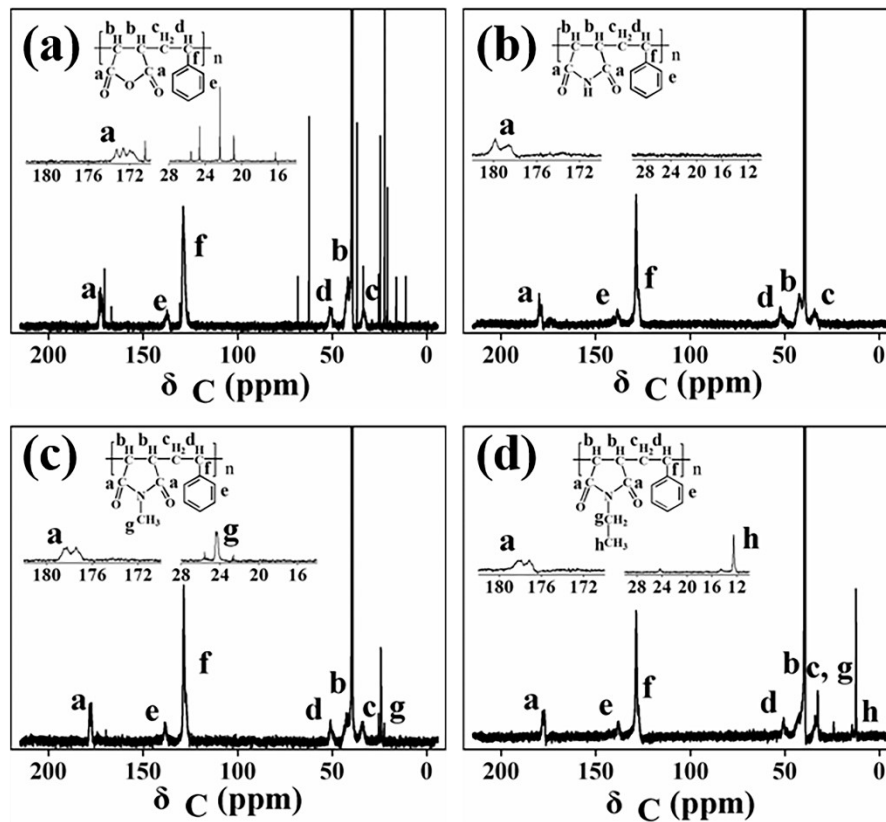


Fig. S8. ^{13}C NMR spectra. (a) SMA, (b) NH_3 -SMI, (c) *N*-methyl SMI and (d) *N*-ethyl SMI.

The ^{13}C NMR spectra of SMA and SMI are shown in Fig. S7. It is clear that the signals assigned to carbonyl were observed at 171.8, 172.4 and 173.1 ppm (Fig. S7.a). These belong to maleic anhydride in SMA. The carbonyl signals would shift to 178.6 and 179.9 ppm in NH_3 -SMI (Fig. S7.b), shift to 177.4 and 178.5 ppm in *N*-methyl SMI (Fig. S7.c) and shift to 177.1 and 178.2 ppm in *N*-ethyl SMI (Fig. S7.d). The chemical shift 24.2 ppm represents $-\text{CH}_3$ attached to the N atom in *N*-methyl SMI, and the chemical shift 12.5 and 14.4 ppm represent $-\text{CH}_2\text{CH}_3$ attached to the N atom in *N*-ethyl SMI. The rest signals representing styrene (138.5 ppm, 129.0 ppm, 52.2 ppm and 34.2 ppm) and $-\text{CH}-$ (42.2 ppm) in maleimide in these spectra were same.

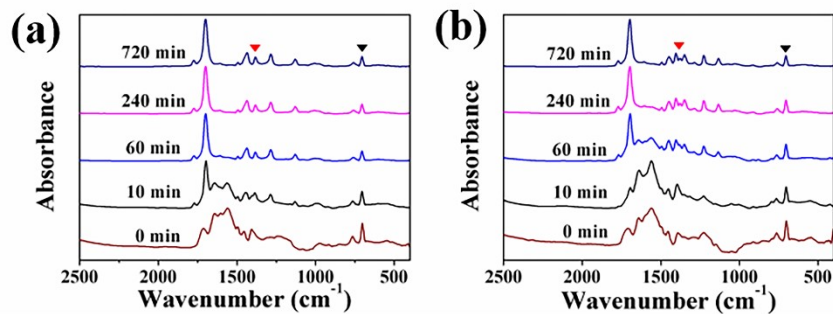


Fig. S9. FTIR spectra of SMAA at different time at 180 °C. (a) *N*-methyl SMAA, and (b) *N*-ethyl SMAA.

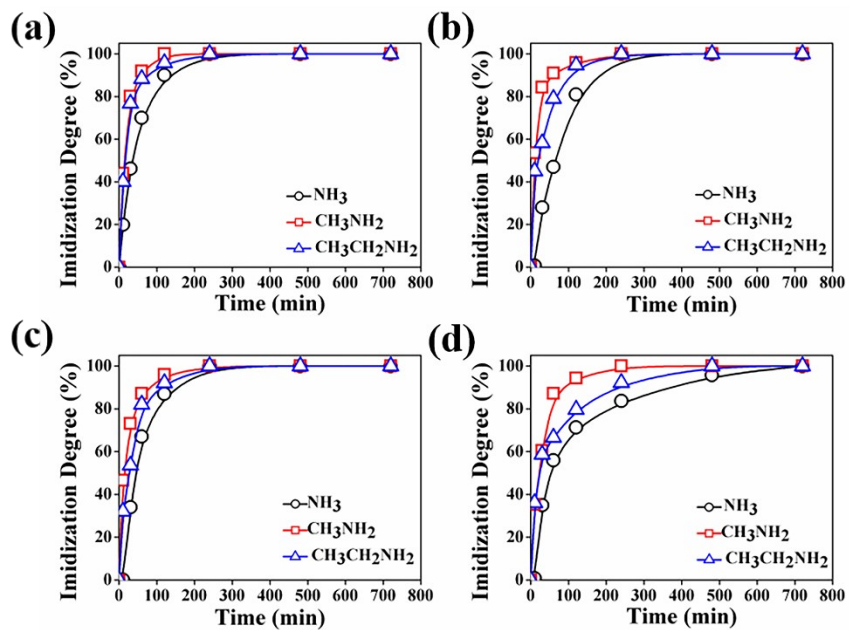


Fig. S10. The imidization degree of SMAA. (a) 226 nm, (b) 452 nm, (c) 534 nm, and (d) 728 nm.

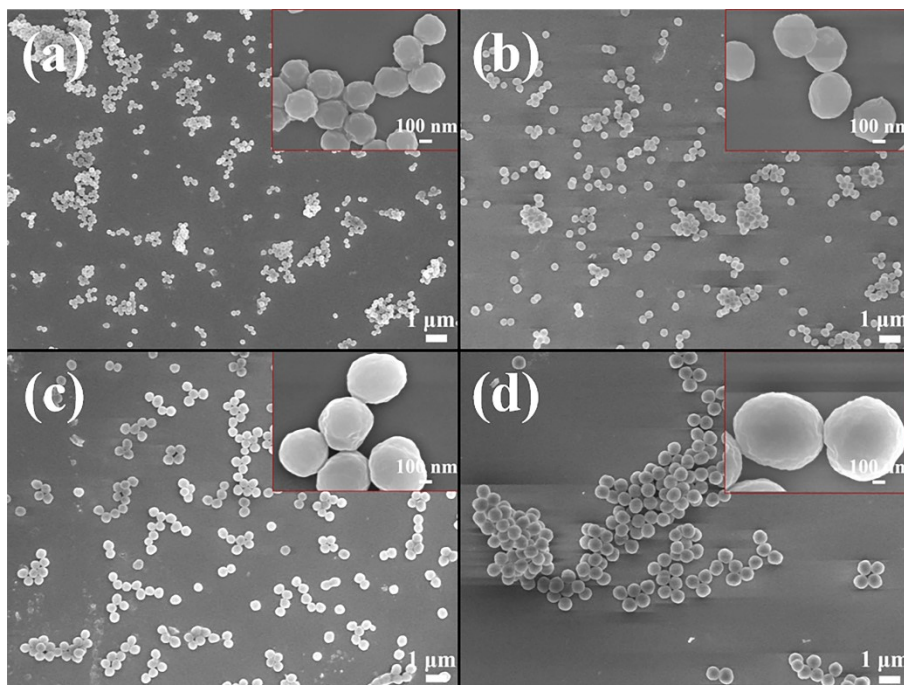


Fig. S11. SEM images of *N*-methyl SMI. (a) 226 nm, (b) 452 nm, (c) 534 nm, and (d) 728 nm.

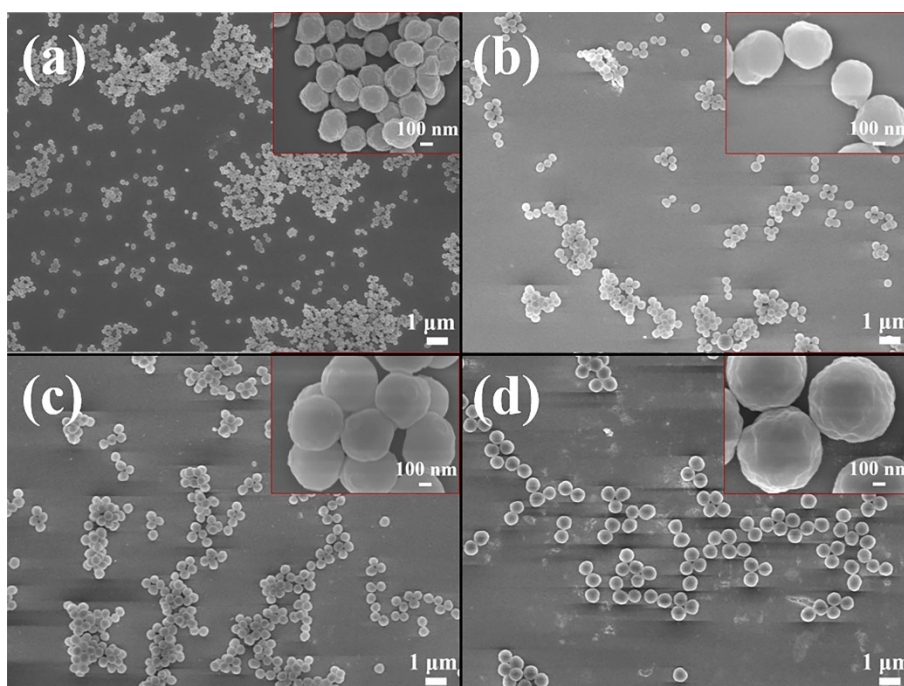


Fig. S12. SEM images of *N*-ethyl SMI. (a) 226 nm, (b) 452 nm, (c) 534 nm, and (d) 728 nm.

Table S3. Diameters of SMAA microspheres.

NH₃		<i>N</i>-methyl		<i>N</i>-ethyl	
\bar{D}/nm	CV/%	\bar{D}/nm	CV/%	\bar{D}/nm	CV/%
222	12.9	230	13.4	226	14.11
452	7.42	456	6.10	460	5.12
531	5.31	530	5.19	528	6.23
724	4.79	728	4.50	735	5.10

Table S4. Diameters of SMI microspheres.

NH₃		<i>N</i>-methyl		<i>N</i>-ethyl	
\bar{D}/nm	CV/%	\bar{D}/nm	CV/%	\bar{D}/nm	CV/%
228	14.9	226	16.4	232	15.11
452	8.98	454	6.10	452	5.42
528	7.10	534	5.19	532	5.23
728	4.47	730	4.60	732	5.20



Fig. S13. The dissolved state of NH_3 -SMI in acetone/water mixture.

Table S5. The ratio of acetone to water in the mixture.

Sample No.	Acetone /g	H ₂ O /g	Acetone : H ₂ O	NH ₃ -SMI/g
1	1	0	5:0	0.2
2	1	0.2	5:1	0.24
3	1	0.4	5:2	0.28
4	1	0.6	5:3	0.32
5	1	0.8	5:4	0.36
6	1	1	5:5	0.4
7	0.8	1	4:5	0.36
8	0.6	1	3:5	0.32
9	0.4	1	2:5	0.28
10	0.2	1	1:5	0.24
11	0	1	0:5	0.2

Mass ratio of NH_3 -SMI to mixed solution (acetone : water) = 20 %.

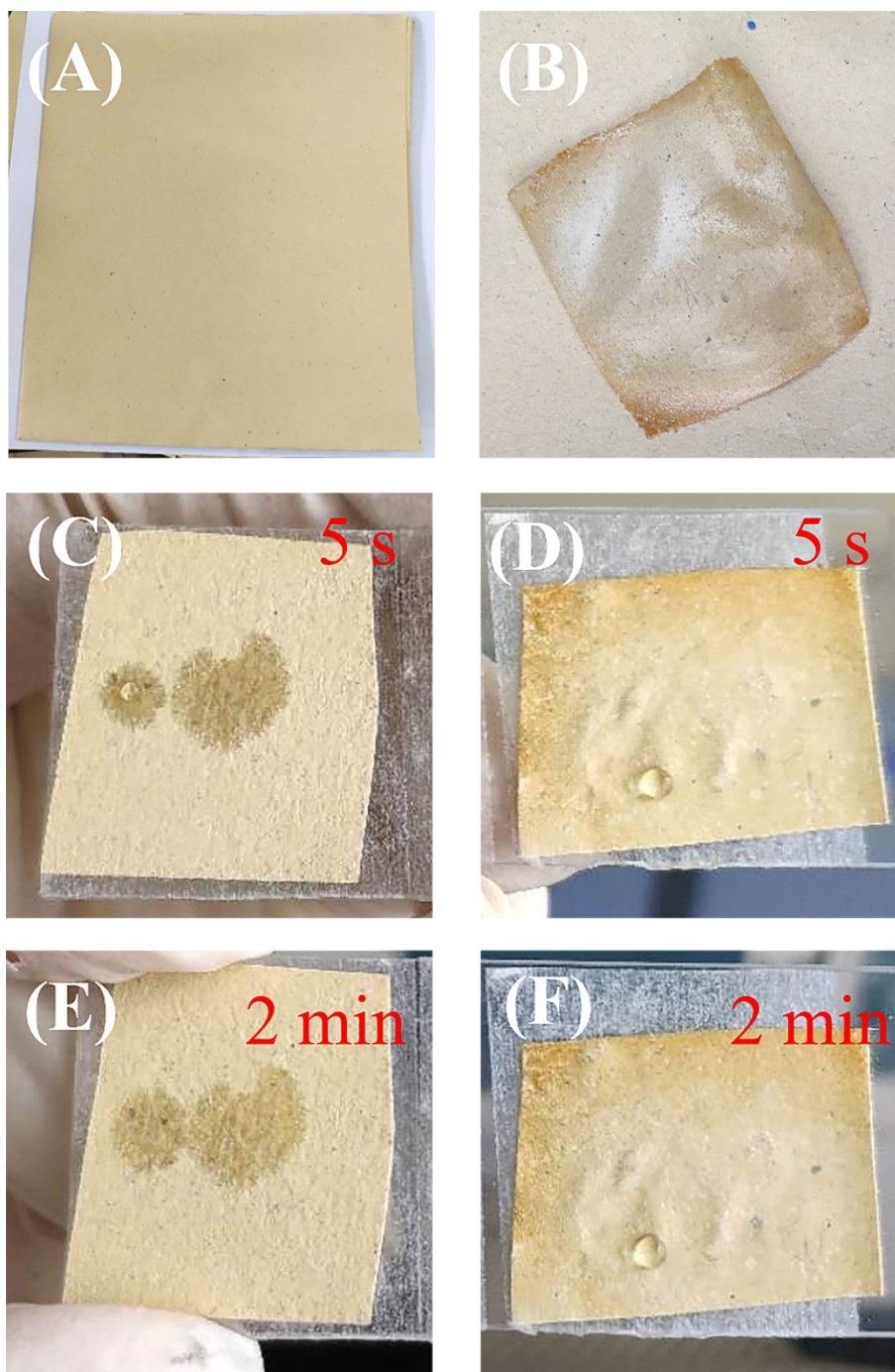


Fig. S14. Photos of uncoated kraft paper (A), kraft paper coated by NH₃-SMI (B) and the presence of water droplets on uncoated kraft paper surface at 5 s (C), kraft paper coated by NH₃-SMI at 5 s (D), uncoated kraft paper surface at 2 min (E) and kraft paper coated by NH₃-SMI at 2 min (F).

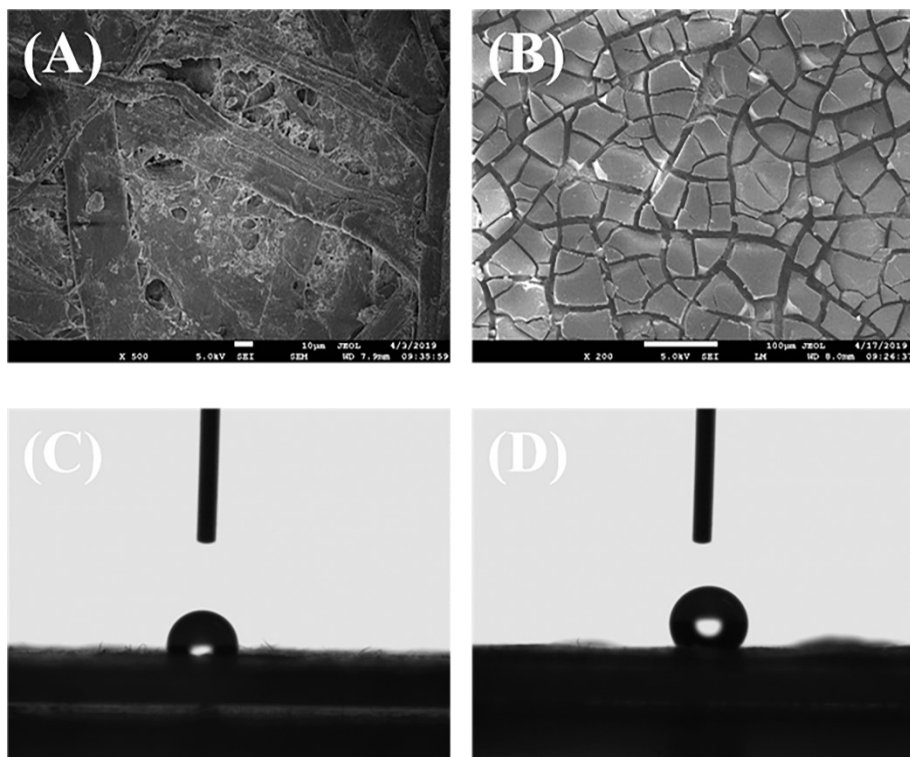


Fig. S15. SEM image of uncoated kraft paper (A) and kraft paper coated by NH_3 -SMI (B), and static water contact angle of uncoated kraft paper (C) and kraft paper coated by NH_3 -SMI (D).